

## Structural variation in the dolomite-ankerite solid-solution series: An X-ray, Mössbauer, and TEM study

RICHARD J. REEDER

Department of Earth and Space Sciences, State University of New York at Stony Brook, Stony Brook, New York 11794, U.S.A.

WAYNE A. DOLLASE

Department of Earth and Space Sciences, University of California, Los Angeles, Los Angeles, California 90024, U.S.A.

### ABSTRACT

Structural variation of the solid-solution series that extends from dolomite to ca. 70 mol%  $\text{CaFe}(\text{CO}_3)_2$  has been examined by using several techniques. Single-crystal X-ray structure refinements for specimens containing 22, 50, and 68 mol%  $\text{CaFe}(\text{CO}_3)_2$  demonstrate essentially full ordering of Ca and the remaining divalent cations. With increasing Fe content, the (Fe,Mg) octahedron dilates at a normal rate while the Ca octahedron shows a small contraction. Both octahedral sites ( $\bar{3}$  symmetry) are trigonally elongated with this small distortion increasing only very slightly with Fe content.

$^{57}\text{Fe}$  Mössbauer spectra of four ankerites [containing 17, 29, 54, and 66 mol%  $\text{CaFe}(\text{CO}_3)_2$ ] show only one moderately split quadrupole doublet with isomer shift of 1.24(1) mm/s. Quadrupole splitting decreases only very slightly from 1.48 to 1.44 mm/s over this range of Fe contents. The Mössbauer data are consistent with  $\text{Fe}^{2+}$  in a single, slightly trigonally distorted, octahedral site whose degree of distortion remains very nearly constant with composition.

Transmission-electron-microscope images and electron-diffraction patterns are compatible with homogeneous microstructures in these samples, all of which have stoichiometric Ca contents. Domain microstructures suggested previously are not present.

The factors that cause natural and synthetic ankerites with compositions exceeding ca. 70 mol%  $\text{CaFe}(\text{CO}_3)_2$  to be unstable (relative to calcite + siderite solid solutions) cannot be obviously identified with any structural parameters so far investigated.

### INTRODUCTION

Fe is probably the most common element substituting in natural dolomites, with  $\text{Fe}^{2+}$  contents reaching approximately 70 mol%  $\text{CaFe}(\text{CO}_3)_2$ . Such ferroan dolomites, or ankerites,<sup>1</sup> nearly always contain small but variable amounts of Mn and less commonly minor Pb and Zn. Compositions of low-Mn ankerites generally lie close to the  $\text{CaMg}(\text{CO}_3)_2$ - $\text{CaFe}(\text{CO}_3)_2$  join (Fig. 1), which lends support to the widely held view that  $\text{Fe}^{2+}$  substitutes principally for Mg. Previous workers have noted that some natural ankerites contain Ca in excess of that required to completely fill the A site (e.g., Goldsmith et al., 1962; Murata et al., 1972). This Ca excess, which can be as large as 8 mol%  $\text{CaCO}_3$ , is similar to that found in many Fe-free dolomites of sedimentary origin (Boles, 1978; Reeder, 1981). Ca-deficient ankerites, like Ca-deficient dolomites, are rare.

The most striking features of this solid solution, however, are the incomplete substitution of Fe for Mg and the apparent nonexistence of the Fe analogue of dolomite,

$\text{CaFe}(\text{CO}_3)_2$ . Experimental studies (Goldsmith et al., 1962; Rosenberg, 1967) as well as compositions of natural samples (Smythe and Dunham, 1947; Goldsmith et al., 1962; Beran, 1975; also see the extensive compilations of ankerite compositions by Essene, 1983, and Anovitz and Essene, 1987) confirm Fe solubility up to, but no greater than, approximately 70 mol%  $\text{CaFe}(\text{CO}_3)_2$ . This restricted solution stands in marked contrast to the complete solution along the  $\text{MgCO}_3$ - $\text{FeCO}_3$  join with end-members magnesite and siderite (Rosenberg, 1963a). Furthermore, several of the experimental efforts cited above have failed to synthesize  $\text{CaFe}(\text{CO}_3)_2$ , and this composition lies within a two-phase field of calcite and siderite solid solutions, at least for temperatures of 350 °C and greater (Goldsmith et al., 1962; Rosenberg, 1963b).

The limited  $\text{Fe}^{2+}$  solubility in the dolomite-ankerite series has long puzzled mineralogists, since it represents a seemingly rare example in which an Mg- $\text{Fe}^{2+}$  substitutional solid solution is not complete. Although considerable experimental work on phase relations in this series has been done, there have been very few crystal-chemical studies that address these interesting problems. Notable, however, is the paper by Rosenberg and Foit (1979) in which the authors suggested that the nonexistence of

<sup>1</sup> Some authors have used the terms *ferroan dolomite* and *ankerite* to distinguish between samples having different Fe/Mg ratios; we use the terms interchangeably here.

$\text{CaFe}(\text{CO}_3)_2$  may be related to excessive distortion of the cation octahedra resulting from  $\text{Fe}^{2+}$  substitution.

The present study was undertaken with the purpose of determining the detailed variations in crystal structure accompanying the substitution of  $\text{Fe}^{2+}$  in dolomite. We report the results of single-crystal X-ray structure refinements, Mössbauer spectroscopy, and TEM observations on a series of ankerites that, when combined with existing data for dolomite, represent nearly the complete range of reported Fe solubility.

### STRUCTURAL CONSIDERATIONS AND PREVIOUS WORK

Ankerites are isostructural with dolomite, having space group  $R\bar{3}$ . Although the primitive unit cell is an acute rhombohedron, it is customary to use a hexagonal description with unit-cell dimensions of ca. 4.8 and 16.0 Å, respectively, for *a* and *c*. A detailed description of the dolomite structure has been given by Reeder (1983), and only essential features are mentioned here. There are two distinct cation sites, designated A and B; both form nearly regular octahedra in which each corner of an octahedron is an oxygen from a different  $\text{CO}_3$  group. The A site is occupied by Ca and the B site by Mg (and Fe) in the ideally ordered case, with layers of Ca octahedra alternating with layers of (Mg,Fe) octahedra along *c*. The octahedra are linked by sharing corners simultaneously with octahedra of the opposite kind and with  $\text{CO}_3$  groups. There is no edge sharing in the structure.

Reeder (1983) summarized the occurrences of double carbonates with the dolomite structure in relation to size differences between the cations. The ordered compounds  $\text{CaMg}(\text{CO}_3)_2$ ,  $\text{CaMn}(\text{CO}_3)_2$ , and  $\text{CaZn}(\text{CO}_3)_2$  occur naturally as the minerals dolomite, kutnahorite, and minrecordite, and  $\text{CdMg}(\text{CO}_3)_2$  has been synthesized as part of several studies (Goldsmith, 1972; Capobianco et al., 1987). The differences in ionic radius between the two cations in each of these compounds are 0.28, 0.17, 0.26, and 0.23 Å, respectively (cf. Reeder, 1983, Table 11, p. 31). It has been pointed out that the cation-ordered arrangement of the dolomite structure is stable only for cation pairs in which significant differences in size exist; in most cases where the ionic radii are similar, a complete solid solution exists (e.g.,  $\text{MgCO}_3$ - $\text{FeCO}_3$ ,  $\text{MnCO}_3$ - $\text{FeCO}_3$ ,  $\text{CaCO}_3$ - $\text{CdCO}_3$ ) rather than an intermediate ordered compound. However, several cation pairs, notably Ca-Fe, do not occur in the dolomite structure and have not been synthesized despite having differences in size that overlap with those for stable pairs. The difference in ionic radius for octahedrally coordinated Ca and  $\text{Fe}^{2+}$  (high spin) is 0.22 Å (Shannon and Prewitt, 1969), which is intermediate between the differences for dolomite and kutnahorite. Thus cation-size considerations, however important, are not solely responsible for stability of the dolomite structure.

Only one X-ray structure refinement for an ankerite has been reported (Beran and Zemmann, 1977; Jarosch, 1985, confirmed their results). This refinement was for a highly ferroan sample with slight Ca excess. Similarly, reported Mössbauer work has been limited to a single

specimen having intermediate Fe content and significant Ca excess (DeGrave and Vochten, 1985).

Complex microstructures observed in TEM, including modulated structures and thin coherent intergrowths, have been correlated with excess Ca in dolomites and ankerites (e.g., Reeder, 1981; Barber and Wenk, 1984; Barber and Khan, 1987). Commonly, such carbonates may also exhibit extra reflections in electron-diffraction patterns as a consequence of reduction in symmetry. Other workers have postulated that many natural ankerites might be composed of nanometer-scale domains with composition  $\text{CaFe}(\text{CO}_3)_2$  intermixed with regions of predominately  $\text{CaMg}(\text{CO}_3)_2$  composition (Kucha and Wieczorek, 1984).

### SAMPLES

Approximately 25 ankerite samples were obtained from various sources for the present study. Electron-microprobe analyses were carried out for most of these samples. In several samples, variations of Fe/Mg were found to occur within individual crystals in the form of growth zoning (also see Beran, 1975). All specimens were found to contain some Mn, and some were found to contain excess Ca. Samples containing Ca in excess of 51 mol%  $\text{CaCO}_3$  were not considered for further study, with the hope of avoiding complications associated with the complex microstructures described above. We note that essentially the same range of Fe solubility occurs for both stoichiometric and Ca-rich natural ankerites. Experimental studies by Goldsmith et al. (1962) at 600 °C and above suggest that slight Ca enrichment is favored for high Fe contents.

Three coarsely crystalline ankerites having different Fe contents were selected for X-ray structure refinement (Table 1). Single crystals were taken directly from regions that had been microprobed. In conjunction with existing refinement data for dolomites, the complete compositional range of Fe solubility in ankerites is represented (Fig. 1). For some of the discussion that follows, we consider the sum of Fe + Mn as the compositional variable, although Mn accounts for less than 3% of total cations in these samples.

Four ankerite samples were selected for the Mössbauer study. Two of these, AMNH 6376 and AMNH 8059, were larger portions of the same samples used for the X-ray study. Limitations of sample size prevented us from using the other X-ray sample for Mössbauer spectroscopy, and consequently two other samples whose Fe contents bracketed that in question were substituted. Compositions of the four Mössbauer powder samples were determined by directly-coupled-plasma atomic-emission spectrometry (Table 1). Slight differences from the microprobe analyses of the two X-ray samples were found, probably due to zoning.

### METHODS

#### X-ray

Precession and Laue photographs of the three crystals revealed sharp reflections without any evidence of split-

TABLE 1. Compositional data for several ankerites

	X-ray specimens			
	BM 1931-294	AMNH 6376	AMNH 8059	
CaCO <sub>3</sub>	0.997	1.007	0.997	
MgCO <sub>3</sub>	0.769	0.451	0.273	
FeCO <sub>3</sub>	0.221	0.502	0.676	
MnCO <sub>3</sub>	0.013	0.040	0.054	
	2.000	2.000	2.000	
Fe + Mn	0.234	0.542	0.730	

	Mössbauer samples			
	AMLI	CAMB-UN	AMNH 6376	AMNH 8059
CaCO <sub>3</sub>	0.994	0.999	0.991	1.018
MgCO <sub>3</sub>	0.831	0.646	0.431	0.279
FeCO <sub>3</sub>	0.171	0.292	0.536	0.656
MnCO <sub>3</sub>	0.004	0.063	0.042	0.047
	2.000	2.000	2.000	2.000

Note: Mole proportion MCO<sub>3</sub> normalized to two total cations. Electron-microprobe data for X-ray specimens; directly-coupled-plasma atomic-emission-spectrometry data for Mössbauer samples. Electron-microprobe data collected on a Cameca Camebax operating at 15 kV with a sample current of 15 nA. Homogeneous carbonate mineral standards were used, and data reduction employed ZAF matrix-correction methods.

ting or streaking. Integrated intensity data ( $\sin \theta/\lambda < 1.19$ ) were collected at 24 °C on an automated Picker four-circle diffractometer using graphite-monochromated MoK $\alpha$  radiation ( $\lambda = 0.7107 \text{ \AA}$ ). Absorption-corrected, symmetry-averaged data were used in the least-squares refinement program in the PROMETHEUS system (Zucker et al., 1983). Crystal and refinement data are given in Table 2, and more complete details of the programs and procedures used are given by Reeder and Markgraf (1986). Unit-cell parameters for these crystals were refined from the centered positions of 24 reflections between 40° and 56° 2 $\theta$ .

### Mössbauer spectroscopy

<sup>57</sup>Fe Mössbauer spectra were obtained at room temperature using a conventional constant-acceleration spectrometer with a Co/Rh source. Samples were prepared by mixing about 100 mg of powdered ankerite with Vaseline to minimize preferred orientation. One half to one million counts per channel were accumulated with peak dips between 50 000 and 100 000 counts. Spectrometer calibration was performed immediately before and after this batch of samples using Fe metal, hematite, ferrous oxalate, and sodium nitroprusside.

## RESULTS

### X-ray structure refinement

**Unit-cell variations.** Hexagonal *a* and *c* cell parameters for the three ankerites are given in Table 2 and are plotted as functions of total Fe + Mn in Figures 2a and 2b. Also included are unit-cell data for a dolomite and for an ankerite studied by Beran and Zemmann (1977). Both *a* and *c* increase in generally linear fashion with increasing Fe substitution as previously found by Goldsmith et al. (1962). As is typical in rhombohedral carbonates, *c* is more strongly affected than is *a*, by a factor of roughly 7. However, the precise compositional dependence of the unit-cell parameters is not fully represented by Figure 2 since Mn and Fe will influence the dimensions differently owing to their different radii. In addition, the site distributions of all four major elements will affect cell dimensions. Goldsmith et al. (1962) accounted for the variation of unit-cell dimensions for the dolomite-ankerite series with a separate term representing each of the major components present, but did not consider the influence of site distributions. Their Equations 1' and 1'' indicate reasonable agreement between our chemical data and unit-cell dimensions.

**Site occupancies.** Occupancies of the A and B sites were refined (Table 3) using constraints of full occupancy and bulk cation chemistry as determined from microprobe analyses (Table 1). Since there are four species (Ca, Mg, Fe, Mn) occupying two distinct sites, a unique site distribution is not possible. To simplify this problem, Fe + Mn were combined as a single species, and Mg, the smallest ion, was assigned to the B site. EPR studies have shown that Mn<sup>2+</sup> is strongly partitioned onto the B site in dolomites, although most specimens contain some Mn<sup>2+</sup> on the A site as well (e.g., Prissok and Lehmann, 1986). By combining Fe and Mn, we implicitly assume that these species will manifest approximately similar site preferences. This may not be strictly correct. Refined site occupancies in kutnahorites (Peacor et al., 1987) suggest that the preference for the B site is stronger for Fe than for Mn. Even so, Mn accounts for less than 3% of total cations in these samples, and since its scattering-factor curve is very similar to that for Fe, there would be little hope of distinguishing between the two.

Refined occupancies (Table 3) show that all three ankerites are nearly completely ordered. That is, the A site is 94% to 99% filled with Ca, with the difference being

TABLE 2. Crystal and refinement data

Sample	BM 1931-294	AMNH 6376	AMNH 8059
Locality	Minas Gerais, Brazil	Goldbrath, Styria, Austria	Erzberg, Styria, Austria
Dimension (mm)	0.20 × 0.21 × 0.18	0.12 × 0.13 × 0.09	0.14 × 0.13 × 0.06
$\mu$ (cm <sup>-1</sup> )	22.46	31.91	37.46
Total obs.	1249	1036	1205
Indep. obs.	821	663	787
<i>R</i>	0.045	0.028	0.016
<i>R<sub>w</sub></i>	0.055	0.031	0.017
<i>a</i> (Å)	4.8116(2)	4.8240(2)	4.8312(2)
<i>c</i> (Å)	16.0421(3)	16.1217(3)	16.1663(3)
<i>V</i> (Å <sup>3</sup> )	321.65(3)	324.91(3)	326.77(3)

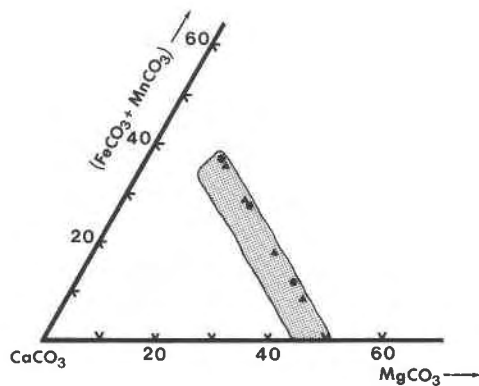


Fig. 1. Portion of the  $\text{CaCO}_3$ - $\text{MgCO}_3$ - $\text{FeCO}_3$  ternary diagram showing approximate compositional range of natural occurrences of dolomite-ankerite solid solutions (shaded region).  $\text{MnCO}_3$ , usually present in small amounts, is included in the  $\text{FeCO}_3$  component. Circles represent the compositions of the three samples used for X-ray structure refinements, and triangles represent samples used in Mössbauer analysis.

made up by Fe + Mn. For the most part, Fe substitutes for Mg in the B site in these samples, in agreement with earlier deductions. Beran and Zemann (1977) also found their high-Fe ankerite to be fully ordered.

**Octahedral bond lengths.** Positional coordinates for atoms and selected interatomic distances for the different polyhedra are given in Tables 4 and 5. Mean M-O bond distances for the A and B octahedra are shown as a function of total Fe + Mn in Figures 3a and 3b. The mean B-O distance increases in a nearly linear fashion with Fe substitution. The rate of increase (the slope) is also in good agreement with other  $\text{Fe}^{2+}$ -Mg solid solutions (cf. Hazen and Finger, 1982, Fig. 8-7).

The mean A-O bond distance shows a small, approximately linear decrease with increasing Fe substitution in the B site. This change is not correlated with slight differences of occupancy in A, which is essentially filled by Ca. Rather the decrease in mean A-O is a consequence of the linkage via corner sharing with  $(\text{Mg,Fe})\text{O}_6$  octahedra and  $\text{CO}_3$  groups. This effect is seen most dramatically by comparing Ca-O and Mg-O distances in dolomite, calcite, and magnesite. In dolomite, each oxygen atom is at a corner shared by a  $\text{CaO}_6$  octahedron and a

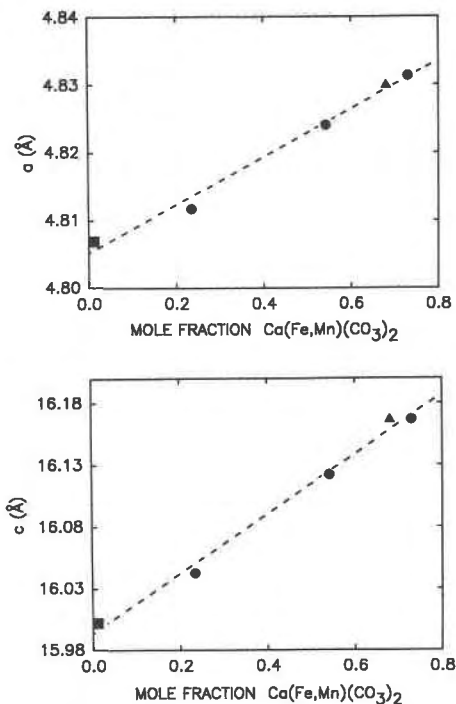


Fig. 2. Hexagonal *a* (a, upper) and *c* (b, lower) unit-cell dimensions for ankerites and a dolomite as functions of increasing Fe + Mn content. The square and the triangle represent a nearly ideal dolomite (Reeder and Markgraf, 1986) and the ankerite of Beran and Zemann (1977), respectively. Errors are less than symbol size.

$\text{MgO}_6$  octahedron (and, of course, a  $\text{CO}_3$  group). In calcite (and magnesite), the equivalent oxygen is shared by two identical  $\text{CaO}_6$  (or  $\text{MgO}_6$ ) octahedra. The inherent disparity between Mg-O and Ca-O bond lengths favors the Mg in dolomite for forming an even shorter (and stronger) bond at the expense of Ca. Thus, the Mg-O distance in dolomite (2.08 Å) is shorter than in magnesite (2.10 Å), and the Ca-O distance (2.38 Å) is longer than in calcite (2.36 Å). In ankerite, the same effect is observed, but to a lesser extent since the mean ionic radius in the B site is always greater than in dolomite owing to the presence of Fe. Predictably then, the A-O distance decreases slightly as the mean B-O distance increases. This steric effect makes it very difficult to estimate site occupancies from mean bond distances, as shown by the refinement data for a largely ordered kutnahorite (Peacor et al., 1987).

The C-O distance is nearly constant in these ankerites at 1.284 Å; this value agrees with the C-O distance found by Beran and Zemann (1977). The displacement of C away from the plane of oxygens, toward the  $(\text{Mg,Fe})$  octahedral layer, apparently decreases with increasing Fe substitution (Table 5).

**Octahedral distortion.** The two cation octahedra in dolomite are trigonally distorted by elongation along the threefold axis. The larger A octahedron is always slightly

TABLE 3. Refined cation-site occupancies

	BM 1931-294	AMNH 6376	AMNH 8059
<b>A site</b>			
Ca	0.944	0.998	0.978
Fe*	0.056(3)	0.002(3)	0.022(2)
<b>B site</b>			
Mg**	0.769	0.451	0.273
Fe*	0.178	0.540	0.708
Ca	0.053	0.009	0.019

\* Mn is included with Fe (see text).

\*\* All Mg was assigned to the B site (see text).

**TABLE 4.** Positional coordinates<sup>1</sup> and temperature factors for three ankerites

	BM 1931-294	AMNH 6376	AMNH 8059
<b>Ca (A)</b>			
$\beta_{11}$	0.0099(2)	0.0105(2)	0.01095(7)
$\beta_{33}$	0.00068(1)	0.00067(1)	0.000663(6)
$B_{\text{eq}}$	0.69(1)	0.72(1)	0.74(1)
<b>Mg, Fe (B)</b>			
$\beta_{11}$	0.0077(2)	0.0078(2)	0.00804(7)
$\beta_{33}$	0.00068(1)	0.00062(1)	0.000633(6)
$B_{\text{eq}}$	0.59(1)	0.59(1)	0.60(1)
<b>Carbon</b>			
<i>z</i>	0.24300(6)	0.24360(6)	0.24395(4)
$\beta_{11}$	0.0080(2)	0.0099(3)	0.0098(1)
$\beta_{33}$	0.00069(2)	0.00070(2)	0.00070(2)
$B_{\text{eq}}$	0.61(1)	0.71(1)	0.70(1)
<b>Oxygen</b>			
<i>x</i>	0.2485(1)	0.2498(1)	0.25045(9)
<i>y</i>	-0.0336(1)	-0.0300(1)	-0.02842(8)
<i>z</i>	0.24426(3)	0.24471(3)	0.24496(2)
$\beta_{11}$	0.0100(2)	0.0098(2)	0.0114(1)
$\beta_{22}$	0.0141(2)	0.0159(3)	0.0161(2)
$\beta_{33}$	0.00114(2)	0.00123(2)	0.00122(1)
$\beta_{12}$	0.0080(2)	0.0073(2)	0.0089(1)
$\beta_{13}$	-0.00065(3)	-0.00024(4)	-0.00076(3)
$\beta_{23}$	-0.00099(4)	-0.00101(5)	-0.00106(3)
$B_{\text{eq}}$	0.89(1)	1.00(1)	1.01(1)

Note: A, B, and carbon sites are on special positions with the following coordinates: A (0,0,0); B (0,0,1/2); carbon (0,0,*z*).  $B_{\text{eq}}$  = equivalent isotropic temperature factor.

more distorted than is B in carbonates with the dolomite structure. Quadratic elongation (QE) values (Robinson et al., 1971) for the ankerites are given in Table 6. By including the QE data for dolomite, it is found that distortion for the  $\text{CaO}_6$  octahedron ranges from a low of 1.0017 for dolomite to a high of 1.0019 for AMNH 8059, the most ferroan ankerite studied. For the  $(\text{Mg,Fe})\text{O}_6$  octahedron, the range is 1.0008 for dolomite to 1.0010 for AMNH 8059. These ankerite values compare well with those from the refinement of Beran and Zemann (cf. Reeder, 1983). Several observations are noteworthy. First, the absolute magnitudes of the distortions involved are very small, and the octahedra are essentially quite regular. Estimated errors for the QE values are given as  $\pm 0.0002$ , but these do not include covariance. Even so, any significant changes in distortion are barely discernible from the present QE data. The changes in O–M–O angles within the octahedra (Table 5) show a trend of increasing trigonal distortion more clearly, but again the absolute change is extremely small. For example, the  $\text{O}_1\text{–Ca–O}_6$  angle (oxygens 1 and 6 are in adjacent layers along *c*) increases from  $92.37^\circ$  in dolomite to only  $92.54^\circ$  in AMNH 8059 and from  $91.66^\circ$  to  $91.80^\circ$  for  $\text{O}_1\text{–(Mg,Fe)–O}_6$ . Nevertheless, some very slight increase in mean distortion occurs with increasing Fe substitution, and by roughly comparable amounts for both octahedra.

#### <sup>57</sup>Fe Mössbauer spectroscopy

Each spectrum shows only one moderately split quadrupole doublet. There is a slight asymmetry to the peaks

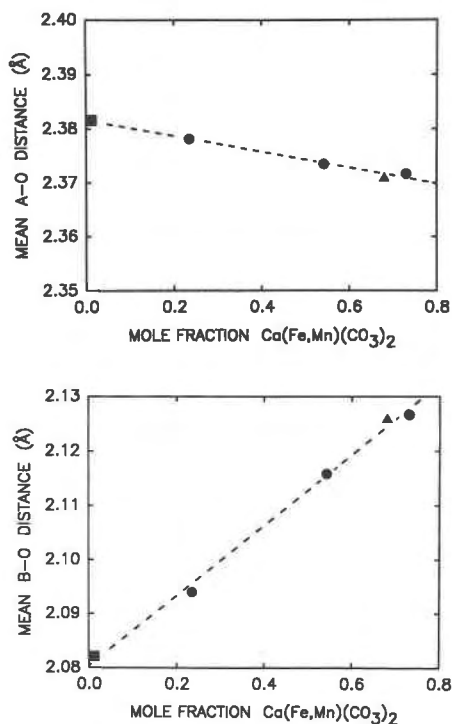


Fig. 3. Mean A–O distance (a, upper) and mean B–O distance (b, lower) for several ankerites and a dolomite as functions of increasing Fe + Mn content. Errors are less than size of symbols, which have same meaning as in Fig. 2.

of this doublet probably due to preferred orientation in the sample (Nagy et al., 1975). There is no evidence of multiple doublets, excessive peak broadening, or other indications of more than one type of site. Spectra were fit with separate peak widths, but the refined values are not statistically different. Final fitted values are given in Table 7.

The quality of the spectral fits are indicated by  $\chi^2$  test and  $\text{MISFIT}$  values given in Table 7. Peak widths are slightly larger than found by DeGrave and Vochten (1985), probably because of a shorter sample-to-source distance. The probable errors of the isomer shifts and quadrupole splittings given in Table 7 are conservatively estimated at  $\pm 0.02$  mm/s based on comparison with standard values taken from the literature.

Isomer shifts (relative to Fe metal) reported elsewhere for carbonates in which  $\text{Fe}^{2+}$  occupies an octahedral site range from a low of about 1.23 mm/s for Fe substituting for Mg to 1.26 and 1.28 mm/s for Fe substituting for Cd and Ca, respectively (Srivastava, 1983). DeGrave and Vochten (1985) reported a room-temperature isomer shift of 1.25 mm/s for an ankerite, although their Figure 5 shows a value closer to 1.23 mm/s. The values obtained in the present study are all  $1.24 \pm 0.01$  mm/s.

The quadrupole splitting is in good agreement with that found by DeGrave and Vochten, consistent with an octahedral site that is only slightly distorted. The range of

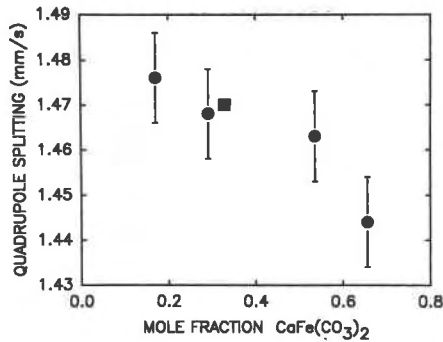


Fig. 4. Quadrupole splitting for several ankerites as a function of increasing Fe content. The square represents the ankerite of DeGrave and Vochten (1985).

quadrupole-splitting values obtained from our four samples barely surpasses the absolute accuracies of the measurements. However, since all spectra were treated in the same manner and were referred to the same instrument calibration, it is likely that the relative error between spectra is considerably smaller, probably about 0.01 mm/s. It is therefore meaningful to plot the measured quadrupole splittings as a function of total Fe content (Fig. 4). The value for DeGrave and Vochten's ankerite is also shown.

The apparent decrease in quadrupole splitting with increasing Fe content parallels the effect of increasing temperature found by DeGrave and Vochten. Considering the rather small trigonal distortion of the octahedral site, such a trend is consistent with a decrease in the degree of distortion of the Fe octahedra. That is, with increasing

TABLE 5. Interatomic distances (Å) and angles (°) for ankerites and a dolomite

	Dolomite*	BM 1931-294	AMNH 6376	AMNH 8059	BZ Ank**
<b>A site</b>					
M-O	2.3816(5)	2.3781(5)	2.3734(5)	2.3716(4)	2.371(1)
O <sub>1</sub> -O <sub>2</sub>	3.298(1)	3.2525(9)	3.283(1)	3.2788(6)	3.277(2)
O <sub>1</sub> -O <sub>6</sub>	3.437(1)	3.4324(9)	3.429(1)	3.4275(6)	3.428(2)
O <sub>1</sub> -M-O <sub>2</sub>	87.63(2)	87.62(2)	87.50(2)	87.46(1)	87.42(5)
O <sub>1</sub> -M-O <sub>6</sub>	92.37(2)	92.38(2)	92.50(2)	92.54(1)	92.58(5)
<b>B site</b>					
M-O	2.0821(5)	2.0939(5)	2.1158(5)	2.1266(4)	2.126(1)
O <sub>1</sub> -O <sub>2</sub>	2.902(1)	2.9164(9)	2.946(1)	2.9598(6)	2.959(2)
O <sub>1</sub> -O <sub>6</sub>	2.987(1)	3.0054(9)	3.037(1)	3.0542(6)	3.053(2)
O <sub>1</sub> -M-O <sub>2</sub>	88.34(2)	88.28(2)	88.25(2)	88.20(1)	88.21(5)
O <sub>1</sub> -M-O <sub>6</sub>	91.66(2)	91.72(2)	91.75(2)	91.80(1)	91.79(5)
<b>CO<sub>3</sub></b>					
C-O	1.2858(5)	1.2843(5)	1.2836(6)	1.2843(4)	1.284(1)
Apl.†	0.017(1)	0.020(1)	0.018(1)	0.0163(8)	0.011(3)
Rot. ∠‡	6.58	6.26	5.60	5.31	5.29

Note: Oxygens labeled according to the scheme given by Reeder (1983); O<sub>1</sub> and O<sub>2</sub> in same layer; O<sub>3</sub> and O<sub>6</sub> in different layers.

\* Data from Reeder and Markgraf (1986) for Eugui dolomite at 24 °C.

\*\* Data from Beran and Zemmann (1977) for their ankerite.

† Aplanarity is the distance (Å) that the C atom is displaced from the plane formed by the three oxygens in a CO<sub>3</sub> group.

‡ Angle (in degrees) by which the C-O bond direction is rotated away from the a axis; i.e., the rotation of the CO<sub>3</sub> group around the threefold axis relative to its position in the calcite structure.

TABLE 6. Octahedral volumes and distortion parameters

	Dolomite*	BM 1931-294	AMNH 6376	AMNH 8059
<b>A site</b>				
V (Å <sup>3</sup> )	17.96(1)	17.887(4)	17.777(4)	17.735(4)
QE**	1.0017(2)	1.0017(2)	1.0018(2)	1.0019(2)
<b>B site</b>				
V (Å <sup>3</sup> )	12.02(1)	12.224(3)	12.611(4)	12.804(3)
QE**	1.0008(2)	1.0009(2)	1.0009(2)	1.0010(2)

\* Data for dolomite from Reeder and Markgraf (1986).

\*\* Quadratic elongation (Robinson et al., 1971).

substitution of Fe for Mg (and/or increasing temperature), the Fe sites become slightly less distorted.

### Electron microscopy and diffraction

Several ion-thinned foils of each of the samples used for X-ray and Mössbauer work were examined using a JEM 200CX transmission electron microscope operating at 200 kV. In addition to checking routinely for anomalous microstructures, particular attention was given to fine details of the selected-area electron-diffraction patterns.

Microstructures in all samples were essentially homogeneous except for only localized defects. Dislocations are typically distributed heterogeneously and generally in very low densities. Several of the specimens contain rare, isolated, fringed defects resembling the coherent ribbonlike intergrowths observed by Barber and Wenk (1984), Barber et al. (1985), and Barber and Khan (1987) in some Ca-rich dolomites and ankerites. Evidence of modulated structures typical of Ca enrichment was absent except for two isolated examples in AMNH 6376 and AMNH 8059. In both these specimens, thin growth zones (~0.5 μm thick) contained irregular contrast modulations. Such zones, however, are volumetrically insignificant.

Selected-area electron-diffraction patterns consistently showed sharp diffraction spots without any evidence of splitting or streaking. Specifically, no *c*-type reflections (cf. Reeder, 1981; Wenk et al., 1983) were observed in any patterns. Specimen BM1931-294 exhibited some mosaic character locally, as evidenced by slight rotations of the diffraction nets.

We also examined several foils of the ankerite sample used by Beran and Zemmann (1977) for their structure refinement. This sample was previously examined with the TEM by Kucha and Wiczorek (1984), who suggested the

TABLE 7. <sup>57</sup>Fe Mössbauer parameters for several ankerites

Sample	IS (mm/s)	QS (mm/s)	Γ (mm/s)	χ <sup>2</sup>	MISFIT
AMLI	1.238	1.476	0.31	0.95	0.0033(6)
CAMB-UN	1.244	1.468	0.32	1.04	0.0023(3)
AMNH 6376	1.234	1.463	0.34	1.09	0.0015(2)
AMNH 8059	1.248	1.444	0.33	1.08	0.0027(4)
Ankerite*	1.24(1)	1.47	0.29-0.30	—	—

Note: Isomer shift = IS (relative to Fe metal); quadrupole splitting = QS; peak width = Γ.

\* Ankerite from DeGrave and Vochten (1985).

presence of a domain structure consisting of 20- to 40-nm domains of  $\text{CaMg}(\text{CO}_3)_2$  and  $\text{CaFe}(\text{CO}_3)_2$ . Our selected-area electron-diffraction patterns for this specimen consistently show sharp diffraction spots without any sign of splitting or extra reflections for orientations comparable to those shown by Kucha and Wieczorek. The splitting required for compositionally distinct domains, such as  $\text{CaMg}(\text{CO}_3)_2$  and  $\text{CaFe}(\text{CO}_3)_2$ , was nowhere in evidence. Furthermore, the diffraction effects shown by Kucha and Wieczorek are consistent with local misorientations of the lattice, or mosaic structure.

## DISCUSSION

The most obvious structural variation upon increasing substitution of  $\text{Fe}^{2+}$  for Mg in ankerites is a dilation of the (Mg,Fe) octahedra at a rate that is comparable to that in many other (Mg,Fe) octahedra. This dilation is accompanied by a weak contraction of the  $\text{CaO}_6$  octahedra (Table 6). Reeder (1983) has pointed out that the principal structural change associated with varying the relative sizes of the A and B octahedra involves their tilting (i.e., rotation) along with that of the  $\text{CO}_3$  groups.

Since the corner-sharing linkage necessarily involves all of these structural units, changes in the A–O and B–O distances require coupled rotations of each. The octahedra and the  $\text{CO}_3$  groups are constrained to rotate around their centers, which lie on triads. The most convenient measure of the net rotations is given by the  $\text{CO}_3$ -group rotation angle, which is taken to be zero at the position assumed in the calcite structure. In dolomite, this rotation angle is  $6.6^\circ$ . Reeder and Wenk (1983) noted that the mean rotation angle decreases as mean ionic radii of ions in the A and B sites become more alike, as in the case of progressive cation disordering. A similar effect is observed in the ankerites in which the mean rotation angle decreases with increasing Fe substitution in the B site (Table 5).

The  $\text{CO}_3$ -group linkage is also important with regard to anisotropy of unit-cell expansion with increasing Fe substitution. The C–O distance is essentially invariant to other changes in the structure, and because the  $\text{CO}_3$  linkage is only within (0001), expansion is preferentially greater along c.

Our observations would seem to be consistent with a well-behaved substitutional solid solution, and they provide no obvious explanation for the limitation in Fe solubility in the dolomite-ankerite series. No structural parameters reach what would appear to be critically large or small values as the maximum Fe content is approached. Mean bond distances and octahedral volume for the B site increase proportionately with increasing Fe substitution (Tables 5 and 6). The range of distances is typical for Mg and  $\text{Fe}^{2+}$  in octahedral coordination. The mean B–O distance for AMNH 8059, containing roughly 70 mol%  $\text{CaFe}(\text{CO}_3)_2$ , is  $2.127 \text{ \AA}$ . This value is almost exactly the distance predicted by linear interpolation between the Mg–O and Fe–O distances in dolomite and siderite, respectively.

Bond distances and octahedral volumes for the A site, filled by Ca, show a slight decrease with increasing Fe substitution in B, but their values always remain intermediate between those for ideal dolomite (A site) and calcite. Moreover, in oxides and silicates, there are many examples of both longer and shorter mean  $^{66}\text{Ca}$ –O distances than found in ankerites.

## Cation ordering

The three ankerite specimens used for the X-ray study are essentially fully ordered, and Fe substitutes almost exclusively for Mg, as expected. The ordering scheme of Ca in the A site and Mg and Fe randomly mixed in the B site apparently remains energetically favored up to the maximum Fe content at  $\sim 70$  mol%  $\text{CaFe}(\text{CO}_3)_2$ . Our present observations are consistent with such a scheme, but we cannot strictly rule out the possibility of some type of Mg–Fe ordering or clustering within the B layers. Clustering that gives  $\text{CaFe}(\text{CO}_3)_2$  and  $\text{CaMg}(\text{CO}_3)_2$  domains on a scale of several 10s of nanometers, as suggested by Kucha and Wieczorek (1984), is highly doubtful on the basis of our TEM observations, as is additional long-range ordering that would reduce the symmetry from  $R\bar{3}$ .

Crystallization temperatures for these three ankerites are difficult to establish. All occur as large aggregates of well-formed rhombohedra and appear to be of hydrothermal vein-filling origin. The two most ferroan samples (AMNH 6376 and 8059) are from the Styrian Erzberg, Austria. On the basis of the experiments of Rosenberg (1967), Beran (1977) estimated crystallization temperatures of between 400 and 500  $^\circ\text{C}$  for ankerites in this area. However, Goldsmith et al. (1962) have emphasized the likelihood of incorporating high Fe contents during metastable ankerite crystallization, and it is possible that much lower temperatures existed.

## The role of octahedral distortion

Despite the attention given to octahedral distortion and its possible influence on stability (cf. Rosenberg and Foit, 1979; Effenberger et al., 1981; Reeder, 1983), we find little evidence to indicate that it is a significant factor limiting Fe substitution in ankerites. Rosenberg and Foit suggested that excessive octahedral distortion might be the cause for the instability of  $\text{CaFe}(\text{CO}_3)_2$  (and the limited Fe solubility in dolomite). They cited a Jahn-Teller effect for  $\text{Fe}^{2+}$  as the likely cause for the distortion. Owing to a lack of precise structural data at the time, Rosenberg and Foit were not able to evaluate and compare the magnitudes of octahedral distortions for different carbonates, as can be done now.

Our refinement results demonstrate that both the A and B octahedra are nearly regular and retain their slight distortions almost unchanged across the entire accessible solid-solution range. When compared with corresponding octahedra in other minerals, those in ankerite and dolomite (and essentially all the rhombohedral carbonates) are nearly always the least distorted. For example, in the compilation of structural data for Ca and (Mg, $\text{Fe}^{2+}$ ) octahedra

given by Smyth and Bish (1988, p. 311), the lowest distortion parameters listed are for dolomite and ankerite octahedra (exceptions are the rock-salt oxides for which the octahedra are ideal). It should also be noted that the  $\text{CaO}_6$  octahedron in our most ferroan ankerite, AMNH 8059, is no more distorted than in calcite ( $QE = 1.0020$ ; Reeder, 1983, Table 2a, p. 11), and it is less distorted than in a largely ordered, natural kutnahorite ( $QE = 1.0022$ ; Peacor et al., 1987). Similarly, the mean  $(\text{Mg,Fe})\text{O}_6$  octahedron in AMNH 8059 is distorted comparably to that in magnesite ( $QE = 1.0009\text{--}1.0010$ ; Reeder, 1983, Table 2a, p. 11) and less than that in siderite ( $QE = 1.0013$ ; Reeder, 1983, Table 2a, p. 11).

Our Mössbauer results confirm that the  $\text{FeO}_6$  octahedra are only slightly distorted in these ankerites. The electric-field gradient is positive both in ankerite (DeGrave and Vochten, 1985) and in siderite (Nagy et al., 1975), confirming the site distortion to be a trigonal elongation. Comparison of our quadrupole splittings, which range from 1.48 to 1.44 mm/s, with those determined for siderite, 1.80 mm/s (Nagy et al., 1975), suggests that the  $\text{FeO}_6$  octahedra are less distorted in ankerite than in siderite, in agreement with the X-ray data. The decrease in quadrupole splitting with increasing Fe content, indicating an increasing regularity, does not necessarily contradict the observed trend in quadratic elongation. Although it is conceivable that in more Fe-rich members, the Fe octahedra become more regular but the average of the Fe and Mg octahedra becomes less regular, it is more likely that the distortion measured by quadratic elongation is only one of the determining contributions to the electric-field gradient. In other words, the two trends apparently measure different aspects of the departure from perfect octahedral symmetry.

It seems that the weak Jahn-Teller effect for high-spin  $\text{Fe}^{2+}$  does not introduce any readily discernible distortion. We cannot comment on a possible dynamic Jahn-Teller effect, which does not introduce any static distortion. A dynamic effect has been suggested for some  $\text{Fe}^{2+}$  octahedra (e.g., Ham, 1965).

#### CONCLUDING REMARKS

Our structural observations demonstrate that natural phases having stoichiometric Ca contents and belonging to the dolomite-ankerite series can be fully ordered. Furthermore, these phases are microstructurally homogeneous, in contrast to Ca-rich dolomites and ankerites. Refinements of the structurally more complex Ca-rich ankerites would be desirable.

X-ray, Mössbauer, and TEM data reveal no obvious indication of a structural instability as maximum observed Fe contents in ankerites are approached. The energetic differences favoring calcite and siderite solid solutions over more ferroan ankerites are apparently more subtle in origin than simply distortion, structural misfit, or cation disorder.

#### ACKNOWLEDGMENTS

Ankerite specimens were kindly provided by the American Museum of Natural History (AMNH samples), the British Museum (Natural History) (BM1931-294), the University of Cambridge Mineralogy-Petrology collection (CAMB-UN), Dr. J.A.D. Dickson, University of Cambridge (AMLI), and Dr. A. Beran, University of Vienna (BZ). X-ray intensity data were collected during a supervised project by B. Comings with assistance from K. Baldwin and J. Paquette. Professor S. McLennan kindly assisted with the DCP analyses, and Dr. P. Bartholomew performed electron-microprobe analysis on one sample and assisted with others. We wish to thank Professor D. H. Lindsley for valuable suggestions during the study and Dr. C. R. Ross II, Professor D. R. Peacor, and Dr. H. Effenberger for their careful reviews of the manuscript. Financial support was provided by NSF grants EAR8416795 and EAR8803423 to R.J.R.

#### REFERENCES CITED

- Anovitz, L.M., and Essene, E.J. (1987) Phase equilibria in the system  $\text{CaCO}_3\text{--MgCO}_3\text{--FeCO}_3$ . *Journal of Petrology*, 28, 389-414.
- Barber, D.J., and Khan, M.R. (1987) Composition-induced microstructures in rhombohedral carbonates. *Mineralogical Magazine*, 51, 71-86.
- Barber, D.J., and Wenk, H.-R. (1984) Microstructures in carbonates from the Alnö and Fen carbonatites. *Contributions to Mineralogy and Petrology*, 88, 233-245.
- Barber, D.J., Reeder, R.J., and Smith, D.J. (1985) A TEM microstructural study of dolomite with curved faces (saddle dolomite). *Contributions to Mineralogy and Petrology*, 91, 82-92.
- Beran, A. (1975) Mikrosondenuntersuchungen von Ankeriten und Sideriten des Steirischen Erzberges. *Tschermaks Mineralogische und Petrographische Mitteilungen*, 22, 250-265.
- (1977) Die Kluftankerite des Steirischen Erzberges und ihre mögliche Verwendung als Geothermometer. *Mineralium Deposita*, 12, 90-95.
- Beran, A., and Zemann, J. (1977) Refinement and comparison of the crystal structures of a dolomite and of an Fe-rich ankerite. *Tschermaks Mineralogische und Petrographische Mitteilungen*, 24, 279-286.
- Boles, J.R. (1978) Active ankerite cementation in the subsurface Eocene of southwest Texas. *Contributions to Mineralogy and Petrology*, 68, 13-22.
- Capobianco, C., Burton, B.P., Davidson, P.M., and Navrotsky, A. (1987) Structural and calorimetric studies of order-disorder in  $\text{CdMg}(\text{CO}_3)_2$ . *Journal of Solid State Chemistry*, 71, 214-223.
- DeGrave, E., and Vochten, R. (1985) An  $^{57}\text{Fe}$  Mössbauer study of ankerite. *Physics and Chemistry of Minerals*, 12, 108-113.
- Effenberger, H., Mereiter, K., and Zemann, J. (1981) Crystal structure refinements of magnesite, calcite, rhodochrosite, siderite, smithsonite, and dolomite with discussion of some aspects of the stereochemistry of calcite-type carbonates. *Zeitschrift für Kristallographie*, 156, 233-243.
- Essene, E.J. (1983) Solid solutions and solvi among metamorphic carbonates with applications to geologic thermobarometry. In R.J. Reeder, Ed., *Carbonates: Mineralogy and chemistry*. Mineralogical Society of America Reviews in Mineralogy, 11, 77-96.
- Goldsmith, J.R. (1972) Cadmium dolomite and the system  $\text{CdCO}_3\text{--MgCO}_3$ . *Journal of Geology*, 80, 611-626.
- Goldsmith, J.R., Graf, D.L., Witters, J., and Northrop, D.A. (1962) Studies in the system  $\text{CaCO}_3\text{--MgCO}_3\text{--FeCO}_3$ : 1. Phase relations; 2. A method for major-element spectrochemical analysis; 3. Compositions of some ferroan dolomites. *Journal of Geology*, 70, 659-688.
- Ham, F.S. (1965) Dynamical Jahn-Teller effect in paramagnetic resonance spectra: Orbit reduction factors and partial quenching of spin-orbit interaction. *Physical Review A*, 6, 1727-1740.
- Hazen, R.M., and Finger, L.W. (1982) *Comparative crystal chemistry*. Wiley, New York.
- Jarosch, D. (1985) Bestätigung der Aplanarität der Karbonatgruppe in Ankerit mit Röntgen-Vierkreisdiffraktometer-Daten. *Anzeiger der Österreichischen Akademie der Wissenschaften, Mathematisch-Naturwissenschaft e. Klasse*, 121, 61-62.



- Kucha, H., and Wieczorek, A. (1984) Evidence for superstructuring in ankerite. *Tschermaks Mineralogische und Petrographische Mitteilungen*, 32, 247–258.
- Murata, K.J., Friedman, I., and Cremer, M. (1972) Geochemistry of diagenetic dolomites in Miocene marine formations of California and Oregon. U.S. Geological Survey Professional Paper 724-C, C1–C12.
- Nagy, D.L., Dézsi, I., and Gonser, U. (1975) Mössbauer studies of  $\text{FeCO}_3$ . *Neues Jahrbuch für Mineralogie Monatshefte*, 1975, 101–114.
- Peacor, D.R., Essene, E.J., and Gaines, A.M. (1987) Petrologic and crystal-chemical implications of cation order-disorder in kutnahorite  $[\text{CaMn}(\text{CO}_3)_2]$ . *American Mineralogist*, 72, 319–328.
- Prissok, F., and Lehmann, G. (1986) An EPR study of  $\text{Mn}^{2+}$  and  $\text{Fe}^{3+}$  in dolomites. *Physics and Chemistry of Minerals*, 13, 331–336.
- Reeder, R.J. (1981) Electron optical investigation of sedimentary dolomites. *Contributions to Mineralogy and Petrology*, 76, 148–157.
- (1983) Crystal chemistry of the rhombohedral carbonates. In R.J. Reeder, Ed., *Carbonates: Mineralogy and chemistry*. Mineralogical Society of America Reviews in Mineralogy, 11, 1–47.
- Reeder, R.J., and Markgraf, S.A. (1986) High-temperature crystal chemistry of dolomite. *American Mineralogist*, 71, 795–804.
- Reeder, R.J., and Wenk, H.-R. (1983) Structure refinements of some thermally disordered dolomites. *American Mineralogist*, 68, 769–776.
- Robinson, K., Gibbs, G.V., and Ribbe, P.H. (1971) Quadratic elongation: A quantitative measure of distortion in coordination polyhedra. *Science*, 172, 567–570.
- Rosenberg, P.E. (1963a) Synthetic solid solutions in the system  $\text{MgCO}_3$ - $\text{FeCO}_3$  and  $\text{MnCO}_3$ - $\text{FeCO}_3$ . *American Mineralogist*, 48, 1396–1400.
- (1963b) Subsolidus relations in the system  $\text{CaCO}_3$ - $\text{FeCO}_3$ . *American Journal of Science*, 261, 683–690.
- (1967) Subsolidus relations in the system  $\text{CaCO}_3$ - $\text{MgCO}_3$ - $\text{FeCO}_3$  between 350° and 550° C. *American Mineralogist*, 52, 787–796.
- Rosenberg, P.E., and Foit, F.F. (1979) The stability of transition metal dolomites in carbonate systems: A discussion. *Geochimica et Cosmochimica Acta*, 43, 951–955.
- Shannon, R.D., and Prewitt, C.T. (1969) Effective ionic radii in oxides and fluorides. *Acta Crystallographica*, B25, 925–946.
- Smyth, J.R., and Bish, D.L. (1988) Crystal structures and cation sites of the rock-forming minerals. Allen and Unwin, Boston.
- Smythe, J.A., and Dunham, K.C. (1947) Ankerites and chalybites from the northern Pennine orofield and the northeast coalfield. *Mineralogical Magazine*, 28, 53–74.
- Srivastava, K.K.P. (1983) Mössbauer quadrupole splitting of  $\text{Fe}^{2+}$  in carbonates. *Journal of Physics C: Solid State Physics*, 16, L1137–L1139.
- Wenk, H.-R., Barber, D.J., and Reeder, R.J. (1983) Microstructures in carbonates. In R.J. Reeder, Ed., *Carbonates: Mineralogy and chemistry*. Mineralogical Society of America Reviews in Mineralogy, 11, 301–367.
- Zucker, U.H., Perenthaler, E., Kuhs, W.F., Bachmann, R., and Schultz, H. (1983) PROMETHEUS. A program for investigation of anharmonic thermal vibrations in crystals. *Journal of Applied Crystallography*, 16, 358.

MANUSCRIPT RECEIVED JANUARY 20, 1989

MANUSCRIPT ACCEPTED JUNE 3, 1989